Chapter 7
Molecular Aspects of Biomineralization of the Echinoderm Endoskeleton

P.U.P.A. Gilbert and Fred H. Wilt

Contents

Abstract Echinoderms possess a rigid endoskeleton composed of calcite and small amounts of occluded organic matrix proteins. The test (i.e., the shell-like structure of adults), spines, pedicellariae, tube feet, and teeth of adults, as well as delicate endoskeletal spicules found in larvae of some classes, are the main skeletal structures. They have been intensively studied for insight into the mechanisms of biomineralization. Recent work on characterization of the mineral phase and occluded proteins in embryonic skeletal spicules shows that these simple-looking structures contain scores of different proteins, and that the mineral phase is composed of amorphous calcium carbonate (ACC), which then transforms to an

P.U.P.A. Gilbert (✉)
Department of Physics, University of Wisconsin-Madison, 1150 University Ave, Madison, WI 53706, USA
e-mail: pupa@physics.wisc.edu

W.E.G. Müller (ed.), *Molecular Biomineralization*, Progress in Molecular and Subcellular Biology 52, DOI 10.1007/978-3-642-21230-7_7,

anhydrous ACC and eventually to calcite. Likewise, the adult tooth shows a similar transition from hydrated ACC to anhydrous ACC to calcite during its formation, and a similar transition is likely occurring during adult spine regeneration. We speculate that: (1) the ACC precursor is a general strategy employed in biomineralization in echinoderms, (2) the numerous occluded proteins play a role in post-secretion formation of the mature biomineralized structure, and (3) proteins with "multi-valent" intrinsically disordered domains are important for formation of occluded matrix structures, and regulation of crucial matrix–mineral interactions, such as ACC to calcite transitions and polymorph selection.

7.1 Introduction

There has been substantial interest in the echinoderm skeleton, especially that of sea urchins, for centuries. Skeletal elements of echinoderms are abundant in the fossil record and, hence, important in paleontology and evolutionary studies. The enveloping shell-like surface, the test, is often admired for its decorative beauty, and for its toughness and strength, which are very different from pure calcite.

The phylum Echinodermata is comprised of five extant classes: sea urchins and sand dollars (echinoidea), sea lilies (crinoidea), sea stars (asteroidea), brittle stars (ophiuroidea), and sea cucumbers (holothuroidea). This phylum and the phylum Hemichordata are the closest relatives of the chordates, which include the vertebrates. Members of these three phyla are the only animals with deuterostome mode of embryonic development, i.e., the site of gastrulation becomes the anal pore of the larva or adult. The echinoderms have a hard, mineralized endoskeleton, which is a composite of calcite and an organic matrix, while the vertebrate endoskeleton uses calcium phosphate.

The sea urchin embryo is well suited for biochemical and molecular studies, and identification and characterization of biomineralization proteins have steadily increased in recent years. There is also intense interest in the mineral phase of skeletal elements in both larva and adult, as well as in the relationships of organic matrix and mineral, and biomechanical properties of the skeletal elements. We shall concentrate in this review on a discussion of recent work on matrix proteins, on relationships of matrix to mineral, and on recent progress in understanding the crystal orientation in skeletal elements, and the mineral precursor phases.

It is not feasible to cite or discuss all the important and pioneering studies on these subjects. Much of the older literature is thoughtfully discussed in books by Simkiss and Wilbur (1989), and by Lowenstam and Weiner (1989). The chapter by Raup (1966) on the echinoderm skeleton is also useful. Work on biomineralization in classes other than echinoids is sparse, and is discussed in a review by Wilt et al. (2003). Decker and Lennarz (1988) have surveyed earlier studies of spicule formation, and Wilt and Ettensohn (2007), and Wilt and Killian (2008) have published reviews of the recent findings on the genes that encode proteins associated with biomineralization in sea urchins.

7.2 Formation of the Endoskeleton in the Embryo

7.2.1 Spicule Formation

The development of the larval endoskeleton in indirectly developing sea urchins (i.e., those that develop through a larval stage) has been studied extensively by embryologists since the late 1800s. The formation of the larval endoskeleton can be followed in real time under the microscope. At the dawning of modern experimental biology, the endoskeletal spicules found in sea urchin larvae were the morphological characters Boveri used in his discovery that chromosomes were the carriers of heredity (Laubichler and Davidson 2008).

The embryology of spicule development has been described in detail by Okazaki (1975a, b), and more recently by Wilt and Ettensohn (2007). At the fourth cell division, four of the resultant 16 cells are clustered at one pole, and are termed micromeres, since they are smaller than the other blastomeres (see Fig. 7.1). At the fifth division, each micromere gives rise to two cells, the larger of which is uniquely dedicated to formation of a skeleton. The so-called large micromeres continue to divide, forming a cohort of 32–64 cells (depending on the species) located in the wall of the vegetal hemisphere of the blastocoel. Just before the invagination movements of gastrulation begin, these micromere descendants, which are epithelial cells, transform into motile mesenchymal cells and burrow through the basement membrane, entering the blastocoel, where they wander, exploring the wall of the blastula for several hours, concomitant with the invagination of the archenteron (primitive gut) during the early phases of gastrulation. These large micromere

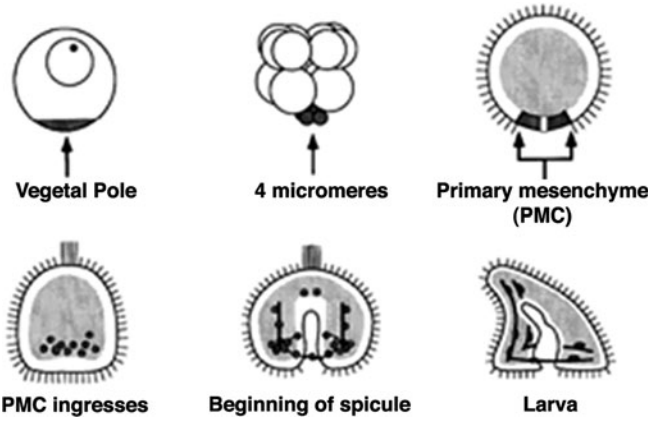

Fig. 7.1 The embryonic development of endoskeletal spicules. Diagrams of several stages are shown, with emphasis on the origin of the spicules. The primary mesenchyme cells and the cytoplasm of the egg from which they derive are black. Spicules are indicated by thick solid lines in the mid-gastrula and pluteus larval stages. The egg is about 100 μm minimum diameter and the larva is about twice that size. Reprinted by permission of Elsevier Publishing from Wilt (1999)

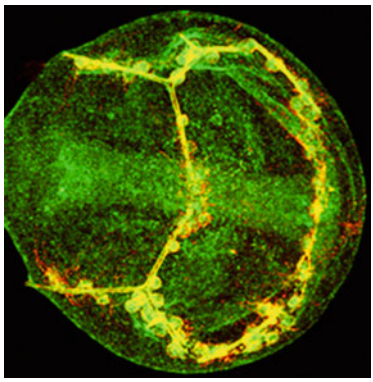

Fig. 7.2 A stained prism-stage embryo. A late prism-stage embryo of *Lytechinus pictus* was stained with an antibody to the spicule matrix protein, LpSM30 (*green*) and with an antibody to a PMC-specific cell surface antigen (*red*). The doubly stained PMC cellular syncytium and spicule are yellow. There is sufficient background staining with the anti-LpSM30 antibody to outline the larva and the developing gut, which runs approximately on the horizontal in this micrograph. The prism-stage embryo is about 180 μm in diameter. Photo courtesy of C.E. Killian and F.H. Wilt

descendants, which are now called primary mesenchyme cells (PMC), then form a stereotypical array in the vegetal portion of the blastocoel, and adjacent PMCs fuse to form a multicellular syncytium, as shown in Fig. 7.2.

The fused PMCs form long cables between cell bodies, and soon after, syncytium formation granules of calcite can be detected in two ventrolateral locations where PMCs are congregated. The embryonic endoskeleton forms by extension of three rays of $CaCO_3$ from each of two calcite rhombohedra, first in a plane defined by the *a* crystallographic axes. The extending spicules, adding mineral principally at the tips and to some extent increasing in girth, then bend to extend in the direction of the *c* axis, and form the elaborate skeleton reminiscent of a Victorian easel; hence, the larva is called a pluteus, Greek for easel (see Fig. 7.2). Okazaki (1975a) devised a method for purification of micromeres, which can then be cultured. They recapitulate the formation of spicules *in vitro* by the same processes and at the same tempo as the intact embryo.

Secondary branches can arise to produce a more elaborate skeleton in many species, and clumps of syncytial PMCs at the extending tip serve as sites of further elongation during larval growth and development (Gustafson and Wolpert 1967). It is important to underline the fact that spicules form only in very close association with the syncytial cables connecting PMC bodies; hence, the macroscopic anatomy of the skeleton is dictated by the positions of the PMCs. The membrane-limited space in which mineral and matrix deposition occurs seems to be entirely enclosed by the cell membrane of the syncytial cables, a seeming vacuole, though more recent studies support the idea that the membrane surrounding the spicule is actually surface plasmalemma that enrobes the spicule; hence, the spicule is a result of vectorial (i.e., directionally secreted) secretion into

a privileged space inside the syncytium that is topologically outside the cell, although it is enrobed by the cell membranes of many PMC cells fused together. A more detailed discussion of this issue can be found in Wilt and Ettensohn (2007) and Wilt (2002).

The morphology of the spicules formed is dictated primarily by PMCs. But the gross anatomical placement of the spicules within the blastocoel depends on the properties of the overlying ectodermal layer of the embryo (Ettensohn and Malinda 1993; Guss and Ettensohn 1997). It has recently been shown that the initiation of calcite formation depends on signaling by the ligand VEGF (Duloquin et al. 2007), which emanates from a small number of ectodermal cells that immediately overlie the congregations of PMCs in the ventrolateral aspects of the blastocoel of the early gastrula stage. A small number of cells that express the homeobox transcription factor, *Otp*, produce the VEGF signal (Dibernardo et al. 1999). PMCs express VEGF receptors for transduction of this ectodermal signal, and initiation and maintenance of calcification depend on this signaling.

7.2.2 Calcium

The calcium of the spicule (and presumably the Mg as well, though it has not been studied) comes from the sea water, as shown by use of isotope studies. (Nakano et al. 1963) Reduction of the Ca concentration of sea water (normal is ~10 mM) below 2–4 mM causes spicules that develop to be malformed. Even lower Ca levels result in irregular, small, mineralized masses, and a generalized deterioration of normal embryonic development (Okazaki 1956). The PMCs must possess very active Ca transporters, presumably with high capacity and low affinity, but they have not been identified or characterized. Beniash et al. (1999) visualized intracellular deposits by electron microscopy that were identified as Ca precipitates, presumably $CaCO_3$. These did not display x-ray diffraction patterns and were believed to be amorphous; after heating of the sample, these deposits diffracted as calcite. After the initiation of triradiate spicule formation, birefringent granules have not been observed in PMCs in living embryos or cultures (see Okazaki 1960); so, either the imported Ca is segregated in intracellular vesicles containing supersaturated Ca solutions, or the precipitated material must be below the resolution of the light microscope, or in a state that is not birefringent.

This role of intracellular calcium deposits was recently addressed by using the Ca fluorophore calcein, a fluorescein derivative that is intensely fluorescent when incorporated into calcium-containing precipitates. Wilt et al. (2008b) used calcein pulse labeling to follow calcium delivery to spicules. They found that brief pulses of calcein-containing sea water, followed by rinsing and culture in normal sea water, resulted in an initial labeling of intracellular submicron sized granules, followed by their clearance from the cell and subsequent appearance of label in developing spicules, particularly near the tips of the extending spicules. They interpreted this as

evidence for an intracellular precipitated, noncrystalline Ca precursor that is shuttled along the syncytial cytoplasmic strand and secreted into the syncytium in which the spicule forms.

7.2.3 Occluded Proteins

Spicule matrix proteins are also synthesized and secreted by PMCs; thereafter, the proteins can be found occluded within the mineral phase. The earlier literature on this subject can be found in the review of Decker and Lennarz (1988). There has been very little work done on the synthesis, delivery, and occlusion of these proteins during spicule formation. Benson et al. (1989) demonstrated, using polyclonal antibodies against an undefined mixture of matrix proteins from the spicule, that intracellular vesicles, which contained putative matrix proteins, could be identified in PMCs. The first matrix proteins studied by modern methods, SM50 and SM30, have been the subject of several studies. Ingersoll et al. (2003) using immunoelectron microscopy and affinity-purified antibodies showed that both of these proteins are found in the Golgi apparatus and in transport vesicles (approximately 50 nm in size), that deliver their contents to the space in which the spicule is formed. Wilt et al. (2008b) followed GFP-tagged versions of SM30 and SM50; in both instances, the PMCs harboring the transgene secreted GFP-tagged SM30/50 into the spicule space near the PMC of origin. This finding contrasts with the delivery of calcium, which shuttles primarily to the extending tip. The kinetics of secretion of ^{35}S-labeled SM30 were followed in PMCs by immunoprecipitation of the protein in the cell and spicule, formed in culture. It took about 20 min after the introduction of label for secreted proteins to begin accumulation in the forming spicule, and the SM30 delivered to the spicule had a somewhat lower molecular mass, indicating that processing of the protein had occurred during the secretion and/or spicule assembly steps.

There are a variety of studies that characterize the cell biology of spicule formation. Inhibitors of metalloproteases stop spicule elongation (Ingersoll and Wilt 1998; Huggins and Lennarz 2001), though this inhibition does not interfere with initial formation of the calcite rhombohedra in the PMCs. It is no surprise that inhibitors of ion transport have a deleterious effect (e.g., Mitsunaga et al. 1986). The mechanism (s) by which vectorial secretion of matrix proteins is accomplished is unknown. We do know that PMCs secrete many other molecules, including collagens and proteoglycans, into the blastocoel (Benson et al. 1990), but such molecules are not found occluded in the spicule, nor are spicule proteins found in the blastocoel.

Finally, it is important to remember that spicule formation may only represent one mode of biomineralization. The biomineral is not assembled on a scaffold at some distance from the cell, as is the case in mollusks, or vertebrate bone, but in intimate contact with the cell. The spicule is completely enrobed by syncytial

membrane and a cytoplasmic sheath without any intervening space, as was shown by Beniash et al. (1997).

7.2.4 Formation of Postembryonic Skeletal Elements

Larvae that survive the rigors of life in the plankton will eventually settle on a suitable substrate, and undergo metamorphosis. The larval structures subsequently wither and disappear, leaving a juvenile sea urchin (Smith et al. 2008). Drawings of advanced larvae show the relationships of the echinus rudiment to the larva more clearly than do microphotographs (see Fig. 7.3). The juvenile urchin forms within the body space, the former blastocoel of the embryo while the growing larva is still part of the plankton. A portion of the larval foregut, in association with cellular descendants of the "small micromeres," which are generated at the fifth cleavage division, gives rise to a rudimentary structure (called the echinus rudiment) that gradually forms a miniature version of the mature sea urchin. The rudiment gradually assumes a more familiar morphology possessing the pentaradial form characteristic of echinoderms. Early in development of the rudiment, small test plates form and become calcified. Tube feet and spines will also become apparent. By the time the juvenile is a few millimeters in diameter, it will have calcified test plate elements, spines, and teeth.

The morphological details of appearance and growth of the adult endoskeleton have been little studied. Some recent work by Yajima and Kiyomoto (2006); (Yajima 2007) has established that cells responsible for juvenile calcified endoskeleton are not PMCs, but rather a related yet distinct embryonic lineage called secondary mesenchyme cells. Smith et al. (2008) worked out a detailed atlas of developmental stages of metamorphosis of *Strongylocentrotus purpuratus* and were able to use specific antibodies directed against endoskeleton-specific proteins to chart the early development of the endoskeleton. Calcified structures in the juvenile are often found arising in close conjunction with larval spicules. Continued development of spines, test plates, and pedicellariae has been studied by electron microscopy (Ameye et al. 1999, 2001). It is generally believed that cells closely associated with biomineralized structures in the adult are responsible for their deposition, a reasonable supposition, though detailed evidence is often lacking, except for the cases of the spine and tooth, which we shall consider in due course.

Classical descriptions of the gross and microanatomy of the juvenile endoskeleton – the test plates, teeth, and spines – can be found in Hyman (1955). The presence in the adult of a few of the characterized matrix proteins of sea urchins has been verified by Western blotting of extracted matrix proteins (Killian and Wilt 1996) or identification of the cognate mRNAs (George et al. 1991; Livingston et al. 2006). Immuno-labelling electron microscopic localization of SM30 and SM50 in pedicellaria and spines of the adult was done by Ameye et al. (1999). We shall restrict subsequent discussion to more recent work on the fine structure of the spicules, the tooth, and the spine.

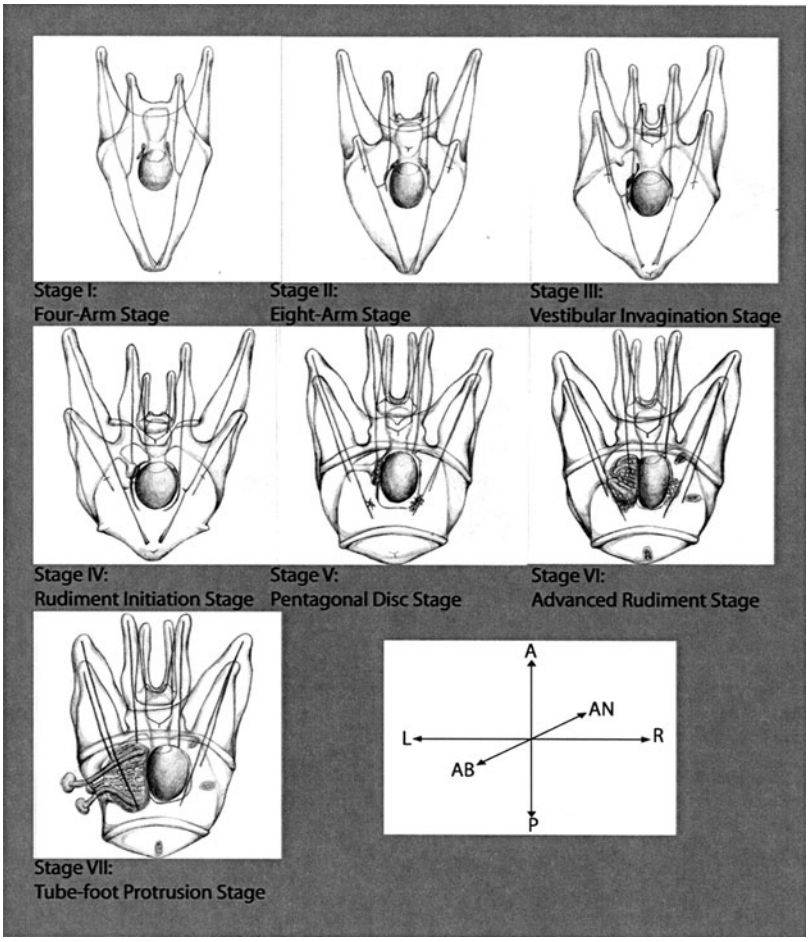

Fig. 7.3 Development of the larva of *S. purpuratus*. Seven stages of development of the pluteus larva during its residence in the plankton. The development of the arms, the skeletal rods, and the gut are emphasized. The echinus rudiment, which will form the juvenile sea urchin after metamorphosis, can be seen emerging from the left side of the midgut in stages V–VII. The body axes are: *L-R* = left-right; *A-P* = anterior-posterior; *AB-AN* = Aboral–Abanal. Reprinted by permission of John Wiley and Sons from Smith et al. (2008)

7.2.5 Recent Work on the Structure and Composition of the Embryonic Spicule

The gross morphology of the endoskeletal spicule in the pluteus stage is a species-specific character. The location of branches, small spurs, and fenestrations is reproducible and specific. Okazaki and Inoue (1976) carried out pioneering work on the orientation of the crystal axes, and showed that the founding mineral granule

appeared as a rhombohedron of calcite. Various workers (Okazaki 1960; Beniash et al. 1997) demonstrated a putative surface "envelope" composed of organic material, and Benson et al. (1983) gave clear morphological evidence for a network of occluded organic molecules in the demineralized spicule. Gentle etching of fractured surfaces revealed a lamellar organization of the mineral, much like growth rings of a section of a tree trunk (Seto et al. 2004). It was proposed that these lamellae could be formed from the periodic deposition of additional layers of mineral that are responsible for increase in girth of the spicule during its development, but there is no direct evidence for that proposal (Seto et al. 2004).

Using affinity-purified antibodies against SM30 and SM50 Seto et al. (2004) showed by immunoelectron microscopy that fractured, etched surfaces were specifically labeled, thereby providing direct evidence for occlusion of these matrix proteins. Both these proteins, especially SM50, are also found on the external surface of the spicule. The picture that emerged is one of well (but not perfectly) aligned domains of calcite (Berman et al. 1993) in which a fibrous network of occluded matrix proteins traverse boundaries between domains.

One goal of research on biomineralization is the identification, enumeration, and function of organic molecules found on, or occluded within, the mineralized structures. Polysaccharides and proteins dominate the lists in the various biomineralized tissues that have been closely examined. Application of the methods of molecular biology has been especially helpful since occluded matrix proteins often resist routine methods of protein purification and characterization. An extended discussion of the approaches and results can be found in reviews by Wilt and Ettensohn (2007) and Killian and Wilt (2008). Suffice it to say that even though the protein content of the sea urchin spicule is very low (~0.1% by mass, Wilt 1999), there are apparently over 40 different proteins of which most, but not all, are acidic and glycosylated[1]. Only one of these 40 has been subjected to a rigorous test of its functional role: synthesis of SM50 during embryonic development is essential for spicule formation (Peled-Kamar et al. 2002; Wilt et al. 2008a). While SM50 is necessary for spicule formation, the exact nature of the role SM50 plays has not been elucidated. It might be instructive to engineer and express counterfeit versions of SM50 to see if particular portions of SM50 can act as a "dominant negative".

The genome of *S. purpuratus* has been sequenced and annotated, and an enumeration of genes known to be involved in spicule formation and/or structure compiled (Livingston et al. 2006). These proteins are mostly acidic, glycosylated, secreted and contain a C-lectin domain. The necessity and/or function of any of them, except SM50, is unknown. We should also remember that proteins important for spicule formation may not necessarily end up occluded in the composite, e.g., the apparent important role of metalloproteases.

[1]Recent proteomic work demonstrated over 200 proteins in the spicule (Mann et al. 2010).

PMC-specific gene expression has also been analyzed by analysis of ESTs of a PMC cDNA library (Zhu et al. 2001). They identified a transmembrane protein, P16, that is essential for spicule formation, as judged by gene knock-down experiments (Cheers and Ettensohn 2005). It is a straightforward matter to use new, powerful methods of protein identification to obtain a complete list of occluded proteins in the spicule, which has been done for the sea urchin tooth and spine (Mann et al. 2008a, b; Mann et al. 2010).

7.3 ACC: Discovery, Importance, and Implications in Other Systems

A resurgence of interest in amorphous minerals was motivated by the discovery by Beniash et al. (1997) that spicules isolated from sea urchin embryos, especially those from earlier stages (e.g., prism) prior to the mature pluteus larva, have substantial amounts of amorphous calcium carbonate (ACC) as identified by Fourier Transform InfraRed (FTIR) spectroscopy. This has been confirmed by a variety of other physical techniques, including visible light polarization and X-ray absorption near-edge structure (XANES) spectroscopy (Politi et al. 2006, 2008). Though stable forms of ACC containing equimolar amounts of hydration water and $CaCO_3$ are known in ascidians, crustaceans, and other animals and plants, (Lowenstam and Weiner 1989), the ACC of the sea urchin embryo slowly transforms to calcite, so that the developing larva (a day or two after attaining the pluteus form) has little ACC. Furthermore, isolated spicules that are stored at $-20°C$ still slowly transform ACC to calcite (Beniash et al. 1997). Synthetic ACC prepared in the laboratory is unstable and quickly transforms to the most stable polymorph, calcite, in minutes, not hours or days.

The ACC found in spicules is apparently not an isolated example. The presence of amorphous precursor minerals was also observed in regenerating spines of sea urchins (Politi et al. 2004), in the forming end of the sea urchin tooth (Killian et al. 2009), in continuously growing fin rays of fish (Mahamid et al., 2008), and in forming tooth enamel from mouse incisors (Beniash et al. 2009). ACC has also been implicated in the formation of mollusk shells (Weiss et al. 2002; Nassif et al. 2005), although a recent report did not find ACC in newly deposited nacre (Kudo et al. 2010). An obvious implication of these diverse findings is that formation of an amorphous phase of the mineral, as a metastable precursor to calcite, aragonite, or carbonated apatite, might be a general tactic used in biomineralization. We shall consider that proposition near the end of this review.

Possible atomic structures of synthetically produced ACC have been investigated using x-ray scattering (Michel et al. 2008; Goodwin et al. 2010), but heretofore the ACC structure has not been investigated in biomineral amorphous precursors. The mode of crystal formation and propagation has been analyzed by Politi et al. (2008) and by Killian et al. (2009). Politi et al. found that there are two

amorphous precursor phases in the sea urchin spicule, one of which is hydrated, and shows spectra exactly equivalent to those of synthetic hydrated ACC. Another phase may be anhydrous ACC, but at the time that work was published, there was no synthetic equivalent to compare the spectra to. The final phase is calcite, as expected, and its spectra are similar to those of geologic and synthetic calcite (Politi et al. 2008). A recent study by Radha et al. (2010) showed that the synthetic anhydrous ACC and spicule ACC have the same enthalpy of transformation into calcite, thus providing strong evidence that the intermediate phase in spicules is indeed anhydrous ACC.

Although echinoderm biominerals behave as single crystals of calcite in polarized light and X-ray diffraction, they do not cleave as crystals. Their fracture surfaces are conchoidal, with curved surfaces and curved edges reminiscent of amorphous glasses. Elegant work by Berman et al. gives compelling evidence that the conchoidal fracture is due to proteins. Calcite rhombohedra were grown in vitro, in the presence of acidic glycoproteins extracted from sea urchin skeletal elements. Not only did the synthetic calcite rhombohedra occlude the proteins, but they also fractured conchoidally (Berman et al. 1988).

This pioneering experiment, and many others that followed it, raise an interesting question: how can a very small amount of organic molecules, e.g., 0.1w% in spicules, make the fracture surface so macroscopically different from a cleavage plane of a crystal? We propose that layers (atomic layers in a crystal or sheets of paper in a sheaf) do not need to be "glued" together extensively. A few spots of "organic glue" between each pair of subsequent layers are sufficient to keep the sheaf or the crystal together, thereby preventing cleavage into separate layers. Hopefully, this hypothesis can be evaluated by obtaining more detailed information about the exact locations of occluded proteins in the skeletal structures discussed here.

7.4 Recent Work on the Adult Spine

The iconic feature of sea urchins is their adornment of spines, which can range from millimeters to scores of centimeters, depending on their location on the test, and on the species. Spines are long and tapered columns of calcite, ending in a sharp point, well designed for defense and abrasion. Their spongy texture provides spaces for several different kinds of dermal cells, and coelomocytes. The surface is covered with an epithelium, meaning that these hard conspicuously external elements are truly endoskeletal.

Figure 7.4 shows the mineralized portion of a spine after bleaching and transverse fracture. The young spine is trabecular and fenestrated, as is the forming test plate. This morphological structure is termed "a stereom." As the spine matures, it becomes more and more heavily mineralized, displaying radially arranged sectors connected by transverse bridges. Sometimes the center is hollow and occupied by cells, sometimes occupied by both cells and extracellular matrix.

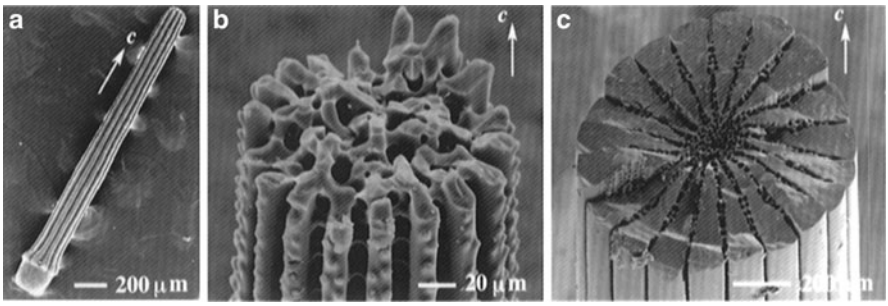

Fig. 7.4 Scanning electron micrographs of secondary spines from the sea urchin *Paracentrotus lividus*. The direction of the c axis of the calcite crystal is indicated by the *arrows*. (**a**) Intact spine. (**b**) Fracture surface of a young spine, showing the spongy structure of the stereom. (**c**) Fracture surface of the mature spine, showing the development of the sectors that filled the stereom. Note the difference in the sizes of the young and mature spines. Data from Aizenberg et al. (1997). Reprinted by permission American Chemical Society

Examination by X-ray diffraction or polarized light demonstrates that the spine is a remarkably co-oriented single crystal, with the *c* crystallographic axis parallel to the long axis of the spine. Figure 7.5 shows a recent result demonstrating that the spine co-orientation is accurate even when observed at much higher resolution with electron diffraction.

Synchrotron X-ray diffraction measurements show that there are domains of perfect crystallinity about 210–235 nm along the long axis (160 nm along the orthogonal transverse axis), and these domains are very well aligned, displaying about 0.130° of variation in alignment of neighboring domains. Geological calcite shows perfect domains of about 800 nm with only 0.003° of misalignment (Berman et al. 1993; Magdans and Gies 2004). The difference between the spine and pure calcite is thought to arise because of the presence of about 0.1w% of occluded organic material (mainly protein) and variable amounts of Mg^{+2} ions (~2–12%) in the calcite of the spine. The Mg content of the calcite is believed to confer additional hardness, and is somewhat higher toward the base of the spine. Mg content can also vary with ocean temperature as well as species.

The structure of the spine at the light and electron microscope level was examined in detail by Heatfield and Travis (1975), looking at the cells in the stereom and epithelial covering as well as the mineral (also, Märkel 1983a, b). The spine elongates by deposition of fenestrated columns of mineral by dermal sclerocytes (sometimes called calcoblasts).

Not much is known about the proteins occluded in the calcite of the spine. Earlier work on occluded proteins of embryonic spicules showed, in passing, that both SM50, and some forms of SM30 are present in the spine Killian and Wilt (1996), and Ameye et al. (1999, 2001) used immunohistochemical methods to demonstrate the presence of both these proteins in forming pedicellariae and spines. More recently, Killian et al. (2009) have used polymerase chain reaction (PCR) to analyze which isoforms of SM30 mRNA are present in spine tissues, and found that

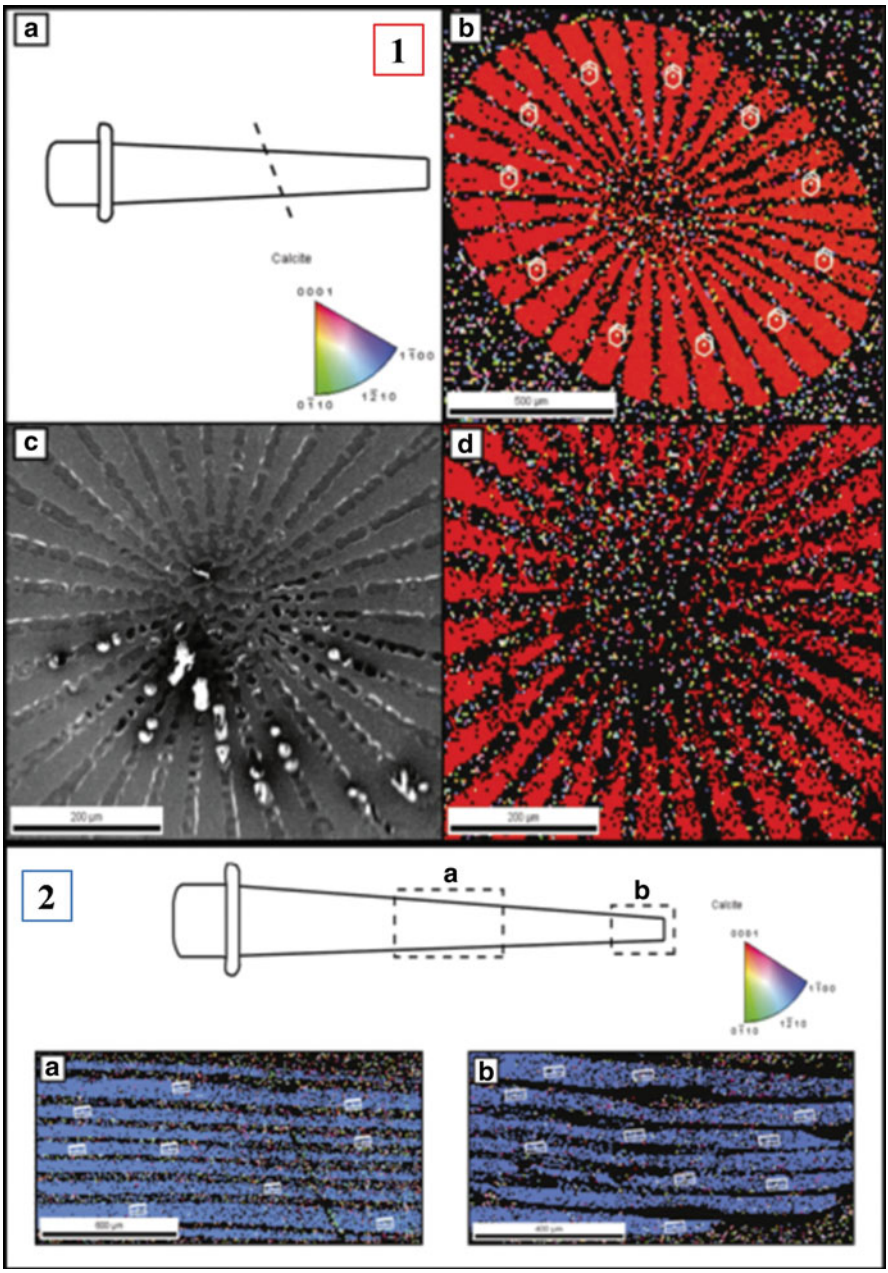

Fig. 7.5 Electron back-scattered diffraction (EBSD) analyses of *P. lividus* spine. (**1**): Transverse and (**2**): Longitudinal cuts. (**1a**): Cartoon of spine with position of section indicated. (**1b**) and (**1d**): EBSD crystallographic orientation map, according to color key in (**1a**), of region presented in (**1c**) as the secondary electron image. Wire frames in (**1c**) indicate that the c-axis is parallel to the spine long axis. (**2**). Cartoon of spine with positions of sections in (**2a**) and (**2b**) indicated. (**2a**) and (**2b**)

SM30 D is dominant, with only low levels of some of the other forms. This is unusual since SM30 D is completely missing in the embryo and is a very minor component in test, teeth, and tube feet. Mann et al. (2008a) have recently published a very thorough proteomic study of the proteins occluded in the spine; there is a very large number, including many of those found in embryonic spicules. SM50, C-lectin-containing proteins, carbonic anhydrase, MSP 130, and proteases were also well represented.

Most of the characterization of spine growth and maturation has been carried out by studying the process of spine regeneration, a process known at least since the mid-nineteenth century. Figure 7.6 depicts the stereom of the tip of a regenerating spine. Elongation of the spine occurs first in the center of existing truncated material by deposition of thin trabeculae; subsequently, lateral "branches" of mineral are laid down and girth is increased. Newly deposited spine is gradually filled in with additional mineral so that the spongy nature of the stereom decreases and prominent columns of calcite dominate. A review of studies of spine regeneration by Dubois and Ameye (2001) provides a good overview of the subject.

The nature of the newly deposited mineral at the tip of a regenerating spine has been studied by Politi et al. (2004). They provided evidence using etching, FTIR, and electron microscopy that the newly deposited mineral is ACC, initially probably in a hydrated form, which is later gradually transformed into anhydrous ACC state, and finally into calcite. This is reminiscent of the findings on the growing tip of the sea urchin embryo spicule, and corroborates the idea that deposition of ACC as a precursor is a general mode of biomineralization of calcite in echinoderms.

7.5 Recent Work on the Adult Tooth

7.5.1 The Mineral Structure of the Sea Urchin Tooth

Sea urchins use their teeth to bite food, but also to burrow into rocks and shelter their bodies from predators (Moore 1966; Nelson and Vance 1979) and from pounding waves (Otter 1932), as seen in Fig. 7.7. In all sea urchins, five teeth are continuously forming at their proximal end (the plumula) and are worn by grinding at their distal end (the tooth tip). They are arranged and supported in a jaw-like apparatus called Aristotle's lantern (Fig. 7.7), as it was first described by Aristotle in his *Historia Animalium*, in 343 BCE.

The tooth structures in several sea urchin species are remarkably similar: the tooth is elongated, slightly curved, approximately 2-cm long, and it has a T-shape cross section (Kniprath 1974; Ma et al. 2008; Märkel and Titschack 1969; Wang

Fig. 7.5 (continued) are EBSD crystallographic orientation maps according to the same color key These maps also indicate that the c-axis is parallel to spine long axis. Data from Moureaux et al. (2010). Reprinted by permission from Elsevier Publishers

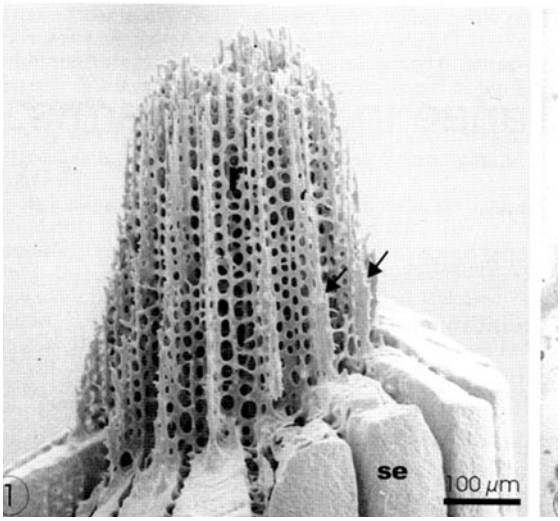

Fig. 7.6 The tip of a regenerating spine. This early stage of a regenerating spine tip shows the fenestrated, reticular stereom of the spine. *Arrows* indicate the presence of lateral bridges between developing columns of calcite sectors. The spine was prepared by chemical debridement of tissue using NaOCl and examined by SEM. Reprinted by permission of John Wiley and Sons from Dubois and Ameye (2001)

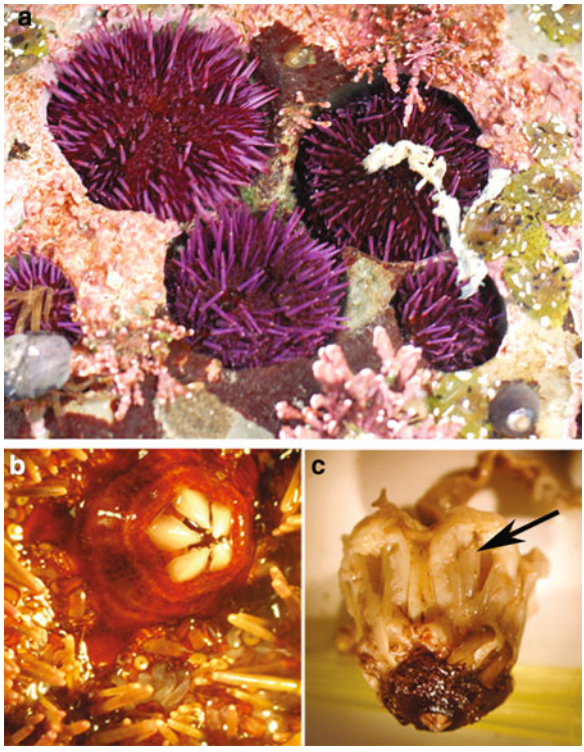

Fig. 7.7 (**a**) Purple sea urchins (*S. purpuratus*) in the intertidal zone at Pt. Arena, California. Notice that each urchin is sheltered into a hole, which it dug into the rock substrate using its teeth. Photo courtesy of C. E. Killian. (**b**) The five tooth tips slowly open and close radially. Photo courtesy of P. Gilbert. (**c**) The Aristotle lantern extracted from the animal, with the tooth tips visible at the bottom, and the side of one tooth indicated by the *arrow*. Photo courtesy of P. Gilbert

et al. 1997; Wang 1998; Ma et al. 2007). The top part of the T is commonly termed the flange; the vertical part of the T is the keel. The flange contains curved calcitic plates, spaced at a few microns from each other. Calcitic fibers with varying

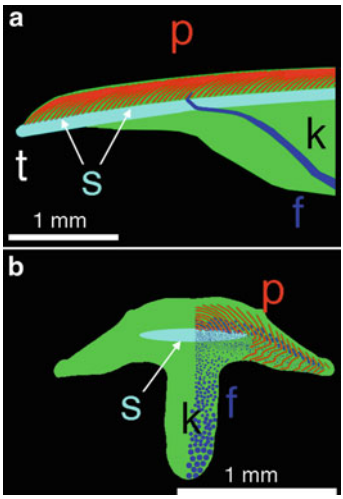

Fig. 7.8 Schematic of a *Strongylocentrotus purpuratus* tooth tip in longitudinal section (**a**) and cross section (**b**). The plates (*p*) are highlighted in *red*, the fibers (*f*) in *blue*. Plates and fibers are cemented together by a polycrystalline matrix (*green*). Notice that the fibers change diameter across the keel (*k*), becoming thicker as they grow away from the plates. The stone part (*s*), highlighted in cyan, is an elliptical region at the center of the tooth cross section, in which the nanoparticles of the polycrystalline matrix reach their highest Mg concentration. At the grinding tip (*t*), the stone part is exposed, after plates and fibers are shed off. Images courtesy of P. Gilbert

diameter start at the ends of the plates, and extend with an S-shape morphology across the keel. Figure 7.8 provides a schematic view of the tooth and its elements.

The five calcitic teeth of an adult sea urchin are continuously growing at a rate of approximately 10 μm per hour at the forming proximal end (Holland 1965; Orme et al. 2001), while the grinding distal end wears off and self-sharpens Killian et al. (2011). The larger structural components of the tooth – plates and fibers – are formed by syncytia of odontoblasts in the plumula at the proximal end of the tooth (Kniprath 1974; Ma et al. 2008), as shown in Fig. 7.9.

As for all other echinoderm biominerals (Brusca and Brusca 1990), the mineralized structures in the sea urchin tooth are highly co-oriented (Berman et al. 1993; Killian et al. 2009). Killian et al. (2009) recently showed that all plates are topologically connected by mineral bridges, thus a single crystal orientation propagates through all plates with spatial continuity. The bridges are shown in Fig. 7.10. Sea urchin species from different oceans possess these same bridges, demonstrating that plate co-orientation via mineral bridges is a highly conserved strategy in biominerals found in sea urchins.

A polycrystalline matrix of ~10 nm particles Yang et al. (2011) of Mg-rich calcite ($Ca_{1-x}Mg_xCO_3$), with x varying between 0.3 and 0.45 in different species (Wang et al. 1997; Killian et al. 2009; Robach et al. 2009), subsequently fills the space between the plates and the fibers, effectively cementing all components together. This matrix was initially believed to be softer (Ma et al. 2007), but

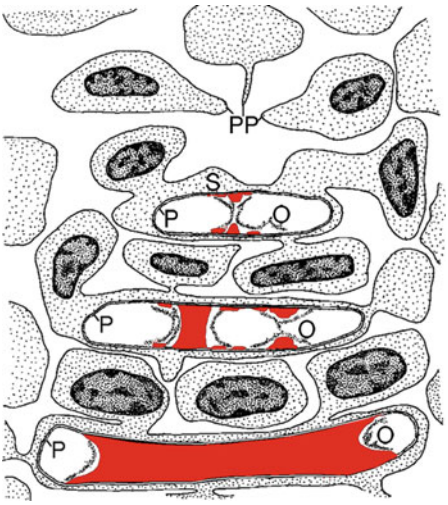

Fig. 7.9 Schematic diagram of the formation of plates in the plumula of the tooth of *P. lividus*. Free odontoblasts (above and at micrograph edges) send the pseudopods (*PP*) to meet and fuse with each other. The plate sheath (*P*) becomes a syncytium, and then calcification (*red*) begins at the two opposite surfaces of the plate sheath. (*O*) is the organic material displaced as the mineral grows and fills the syncytium. Adapted from Kniprath (1974) by permission of Springer Verlag

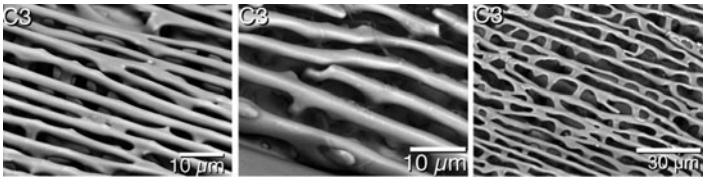

Fig. 7.10 The mineral bridges connecting the plates in the Pacific *S. purpuratus* (*left*), the Mediterranean *P. lividus* (*center*), and Atlantic *L. variegatus* (*right*). Data from Killian et al. (2009). See the original publication and its supporting information to visualize the location of the bridges on the sides of the flange. By permission of American Chemical Society

recently found to be harder (Ma et al. 2008) than plates and fibers. It is clear from Fig. 7.8a that it is the polycrystalline matrix in the stone part that becomes the sharp, hard tip of the tooth that does the grinding.

Recently, Ma et al. (2009) reported that the polycrystalline matrix is highly co-oriented in *P. lividus*. Furthermore, Robach et al. (2009) demonstrated that polycrystalline matrix and fibers share the same orientation in *L. variegatus*, whereas Killian et al. (2009) and Yang et al. (2011) made the same observation in *S. purpuratus*. These concurring observations raise an important question: how does the polycrystalline matrix form and co-orient its crystal nanoparticles? Are the nanoparticles aggregating before or after crystallizing? In other words, is this the result of oriented attachment of crystalline nanoparticles, as first observed by Penn

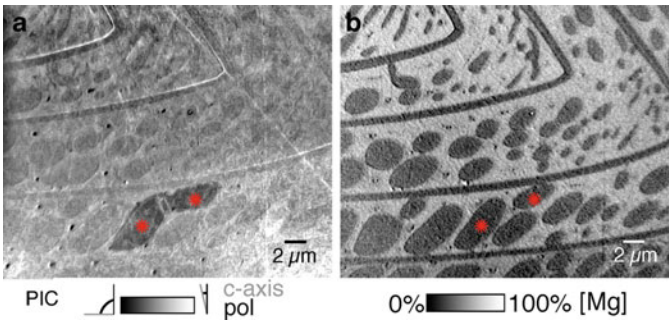

Fig. 7.11 Two stray fibers reveal how co-orientation arises. Spectromicroscopy results from a region of a cross section at the mature end of an *S. purpuratus* tooth. (**a**) Map in which gray level indicates crystal orientation. This map shows two strongly misoriented fibers (red asterisks). (**b**) Mg distribution map from the same region in A, showing well-defined and sharp elliptical fiber edges. Such strongly misaligned fibers are extremely rare in the sea urchin tooth, in which all other fibers are co-oriented with each other and with the polycrystalline matrix. Despite the sharp edges of the fibers in the Mg map, the map in A shows that the polycrystalline matrix surrounding and between the two stray fibers is as misoriented as the fibers themselves. This indicates that the nanoparticles in the polycrystalline matrix get their orientation from the fibers. Data from Killian et al. (2009). By permission of American Chemical Society

and Banfield in TiO_2 (Penn and Banfield 1999), and FeOOH (Banfield et al. 2000), and later in many other synthetic mesocrystals (Cölfen and Antonietti 2008)? Or, is this the result of an amorphous precursor phase forming first, with crystallinity propagating through it subsequently (Aizenberg et al. 2003; Politi et al. 2008)?

This question was addressed in detail by Killian et al. (2009), who showed that, indeed, amorphous precursor phases are aggregated first, and then crystallinity propagates through them via a mechanism of secondary nucleation. Figure 7.11 shows the propagation front of crystallinity and crystal orientation, starting from the fibers and expanding into the surrounding polycrystalline matrix.

Interestingly, spectroscopic analysis at the forming end of the *S. purpuratus* tooth revealed for the first time that there are not one but two amorphous precursor minerals (Killian et al. 2009). These precursor phases are identical to those reported by Politi et al. (2008) in *S. purpuratus* larval spicules. The phases are hydrated ACC, crystalline calcite, and another phase, which is presumably intermediate, and presumably anhydrous ACC, although the order in which the phases occur during tooth formation is unclear and difficult to detect. The aforementioned microcalorimetry results by the Navrotsky group indicate that the enthalpy of transformation from dehydrated synthetic ACC and calcite is very similar to that of forming spicules. This similarity provides the first evidence, to the best of our knowledge, that in sea urchin spicules the temporal sequence of phases is hydrated ACC → anhydrous ACC → calcite. In addition, the microcalorimetry data confirm that this sequence is thermodynamically exothermic, and thus energetically downhill (Radha et al. 2010). We predict that the same sequence of transformations takes place in the tooth.

7.5.2 *Matrix Proteins of the Tooth*

The tooth elements are also known to contain organic material occluded in the calcite. The entire mineralized portion of the tooth, ground and cleaned of adherent material with NaOCl, has been subjected to proteomic analysis by Mann et al. (2008b). Some 138 proteins were identified, 56 of which had been previously identified by this group in test and spine. Major components were identical to abundant proteins in test and spine, while some apparent tooth-specific proteins were especially rich in alanine and proline.

Killian et al. (2010) using PCR methods demonstrated that mRNA encoding SM30 E was very prominent both in mineralized portions and the plumula, and earlier work showed that SM50 is present. Recent work by Veis and his collaborators (Alvares et al., 2009) has identified a number of occluded phosphoproteins. Two of them are identical to proteins identified in an EST library of PMCs of the embryo, notably P16 and P19. P16 had been shown by Cheers and Ettensohn (2005) to be a transmembrane protein whose function was essential for embryonic spicule deposition. Alvares et al. (2009) showed using specific antibody staining that P16, dubbed UTMP16 in the tooth, is found in syncytial membranes in contact with mineral. Mann et al. (2010) have recently analyzed the tooth proteome for the presence of phosphoproteins; they found 15 phosphorylated proteins, 13 of which are unique to tooth tissue.

One of these, named phosphodontin, is rather prominent and contains 35 repeats of an acidic 11–12 amino acid motif that is phosphorylated. Though the amino acid sequence is not orthologous to any known vertebrate tooth protein, the sequence and charge of the peptides indicate it is probably an intrinsically disordered protein.

7.6 Generalizations

Biomineralization processes in Echinoderms display certain general features. Mineralization proceeds in privileged spaces closely apposed by cellular processes, i.e., surrounded by phospholipid membranes. Large numbers of proteins, many of which (but not all) are acidic glycoproteins, are secreted into this space, and ACC, perhaps in the hydrated form, is also deposited into the same places. The ACC gradually transforms to calcite, and some of the proteins are occluded within the forming skeletal element. The details of initial assembly of ACC and protein are not clear, but the slow conversion of ACC to calcite probably occurs by some atomic level reorientation of anhydrous ACC to calcite via a secondary nucleation type of propagation, presenting, at least temporarily, a patchwork of ACC and calcite.

In some respects, this is not so different from proposals made by others (Veis 2008): in this view, cells construct a structural matrix in a defined space, other molecules then assist in orderly nucleation and regulation of crystal growth, habit, shape, and size. One could argue that formation of shells in the extrapallial space

adjoining the mantle of mollusks utilizes similar processes. These generalizations, while providing a useful viewpoint, do not easily lead to experimentally testable models. Just what are the matrix molecules? How do they participate? What molecules preside over regulation of the transition from ACC to calcite or aragonite? Of amorphous calcium phosphates to carbonated apatite? How is the secretion of molecules linked to attaining particular crystalline polymorphs?

New facts have emerged that may help inform some models. In our judgment, these are:

1. Amorphous forms of the mineral can and do serve as precursors,
2. Very large numbers of protein-modifying enzymes are occluded in the amorphous mineral and could regulate transitions to crystalline state, polymorph selection, resistance to fracture, and other properties of the crystal,
3. While there are few, if any, orthologs of occluded "matrix" proteins present in shells, stereoms, or vertebrate teeth and bones, proteins with intrinsically disordered domains play a crucial role in regulation of nascent mineralization.

We have already touched on the first point, and while the presence of an amorphous precursor has not been shown to be near-universal, the examples have been reported from three different phyla: echinoderms (Beniash et al. 1997; Politi et al. 2004, 2008; Killian et al. 2009), mollusks (Weiss et al. 2002; Nassif et al. 2005), and chordates (Mahamid et al. 2008; Beniash et al. 2009). Thus the idea of generalizing amorphous precursors is not unreasonable. Indeed, it helps explain how crystalline biominerals can attain the wide variety of shapes that they do. It should be noted, however, that Kudo et al. (2010) did not observe ACC in nacre deposition in the Japanese oyster, *Crassostrea nippona*.

The second point is hinted at in the recent proteomic studies of echinoderm teeth, test, and spines. An extraordinary number of different proteins are occluded; many of them are present in amounts that are unlikely to be due to contamination, and indeed, were identified earlier by methods with less resolution (Killian and Wilt, 1996). Of course, the presence of some organic components could be due to contamination. Mann et al. (2008b) did compare protein content of ground tooth fragments with and without treatment with NaOCl. The intentional "contamination" indicated that many of the proteins provisionally classified as "occluded" (such as carbonic anhydrase, metalloproteases, cyclophilins) are probably authentic occluded proteins, although some very rare ones (e.g., histones) are more likely contaminants. Therefore, the putative presence of proteases, e.g., indicates that post-secretory modifications of matrix proteins can and probably do occur, and thus, could be expected to participate in the regulation of changes in the mineral phase.

Third, and finally, there is now enough genomic information from vertebrates, from the sea urchin, and from some mollusks and invertebrates, to prudently conclude that major matrix proteins from one clade are not present in others. For instance, the SM30 and SM50 protein families of echinoderms are not found in mollusks or vertebrates. Dentinal phosphoproteins of vertebrate teeth are not found in echinoderms or mollusks, and so on. What does emerge, however, is the presence of proteins in mollusks, (AP24, Pif, n16, etc.), echinoderms, and vertebrates

(Sibling family proteins) that have extended domains termed "intrinsically disordered" and can adopt different conformations when interacting with different "targets", such as crystal surfaces. Such proteins have been shown to participate in polymorph selection (aragonite/calcite) in mollusks (Evans 2008; McMahon et al. 2005; Metzler et al. 2010). In addition to IDP domains, domains with dense clusters of negative charge, such as phosphates found in phosphophoryn of dentin, could conceivably play similar roles in different biomineralizing systems. Perhaps we should look for analogous function of certain domains, rather than specific proteins, as a common thread in biomineralization.

There has been a radical shift in the kinds of models considered to explain the formation of biominerals. Just a few decades ago, it would have been difficult to foresee amorphous precursors and proteins with domains of poorly defined conformation playing roles in biomineralization, but these are now well established. There are exciting developments before us. Current research is so robust that we can foresee considerable progress in the near future.

Acknowledgments The authors gratefully acknowledge support for research in their respective laboratories from DOE grant DE-FG02-07ER15899, NSF grant DMR&CHE-0613972, and UW-Madison Hamel Award to PUPAG, and NSF grant 0444724 and Committee on Research of UC Berkeley to FW.

References

Aizenberg J, Hanson J, Koetzle TF, Weiner S, Addadi L (1997) Control of macromolecule distribution within synthetic and biogenic single calcite crystals. J Am Chem Soc 119:881–886

Aizenberg J, Muller DA, Grazul JL, Hamann DR (2003) Direct fabrication of large micropatterned single crystals. Science 299:1205–1208

Alvares K, Dixit SE, Lux E, Veis A (2009) Echinoderm phosphorylated matrix proteins UTMP16 and UTMP19 have different functions in sea urchin tooth mineralization. J Biol Chem 284:26149–26160

Ameye L, Hermann R, Wilt F, Dubois P (1999) Ultrastructural localization of proteins involved in sea urchin biomineralization. J Histochem Cytochem 47:1189–1200

Ameye L, Becker G, Killian C, Wilt F, Kemps R, Kuypers S, DuBois P (2001) Proteins and saccharides of the sea urchin organic matrix of mineralization: characterization and localization in the spine skeleton. J Struct Biol 134:56–66

Banfield JF, Welch SA, Zhang HZ, Ebert TT, Penn RL (2000) Aggregation-based crystal growth and microstructure development in natural iron oxyhydroxide biomineralization products. Science 289:751–754

Beniash E, Aizenberg J, Addadi L, Weiner S (1997) Amorphous calcium carbonate transforms into calcite during sea urchin larval spicule growth. Proc R Soc Lond Biol 264:461–465

Beniash E, Addadi L, Weiner S (1999) Cellular control over spicule formation in sea urchin embryos: a structural approach. J Struct Biol 125:50–62

Beniash E, Metzler R, Lam RSK, Gilbert PUPA (2009) Transient amorphous calcium phosphate in forming enamel. J Struct Biol 166:133–143

Benson S, Jones EME, Benson N, Wilt F (1983) Morphology of the organic matrix of the spicule of the sea urchin larva. Exp Cell Res 148:249–253

Benson NC, Benson SC, Wilt F (1989) Immunogold detection of glycoprotein antigens in sea urchin embryos. Am J Anat 185:177–182

Benson S, Smith L, Wilt F, Shaw R (1990) Synthesis and secretion of collagen by cultured sea urchin micromeres. Exp Cell Res 188:141–146

Berman A, Addadi L, Weiner S (1988) Interactions of sea-urchin skeleton macromolecules with growing calcite crystals-a study of intracrystalline proteins. Nature 331:546–548

Berman A, Hanson J, Leiserowitz L, Koetzle TF, Weiner S, Addadi L (1993) Biological control of crystal texture: a widespread strategy for adapting crystal properties to function. Science 259:776–779

Brusca RC, Brusca GJ (1990) Invertebrates. Sinauer Associates, Sunderland, MA

Cheers MS, Ettensohn CA (2005) P16 is an essential regulator of skeletogenesis in the sea urchin embryo. Dev Biol 283:384–396

Cölfen H, Antonietti M (2008) Mesocrystals and nonclassical crystallization. John Wiley & Sons, Chichester, UK

Decker GL, Lennarz WJ (1988) Skeletogenesis in the sea urchin embryo. Development 103:231–247

Dibernardo M, Castagnetti S, Bellomonte D, Oliveri P, Melfi R, Palla F, Spinelli G (1999) Spatially restricted expression of *Pl OTP* of *P. lividus* orthopedia related homeobox gene, is correlated with oral ectoderm patterning and skeletal morphogenesis in late cleavage sea urchin embryos. Development 126:2171–2179

DuBois P, Ameye L (2001) Regeneration of spines and pedicellariae in Echinoderms: a review. Micros Res Tech 55:427–437

Duloquin L, Lhomond G, Gache C (2007) Localized VEGF signaling from the ectoderm to mesenchyme cell controls morphogenesis of the sea urchin embryo skeleton. Development 134:2293–2302

Ettensohn CE, Malinda KM (1993) Size regulation and morphogenesis: a cellular analysis of skeletogenesis in the sea urchin embryo. Development 119:155–167

Evans JS (2008) "Tuning in" to mollusk shell nacre- and prismatic-associated protein terminal sequences: Implications for biomineralization and the construction of high performance inorganic-organic composites. Chem Rev 108:4455–4462

George NC, Killian CE, Wilt FH (1991) Characterization and expression of a gene encoding a 30.6 kD *Strongylocentrotus purpuratus* spicule matrix protein. Dev Biol 147:334–342

Goodwin AL, Michel FM, Phillips BL, Keen DA, Dove MT, Reeder RJ (2010) Nanoporous Structure and Medium-Range Order in Synthetic Amorphous Calcium Carbonate. Chemistry of Materials 22:3197–3205

Guss KA, Ettensohn CA (1997) Skeletal morphogenesis in the sea urchin embryo: regulation of primary mesenchyme gene expression and skeletal rod growth by ectoderm-derived cues. Development 124:1899–1908

Gustafson T, Wolpert LM (1967) Cellular movement and contact in sea urchin morphogenesis. Biol Rev 42:441–498

Heatfield BM, Travis DF (1975) Ultrastructural studies of regenerating spines of the sea urchin *Strongylocentrotus purpuratus* I. Cell types without spherules. J Morphol 145:3–50

Holland ND (1965) An autoradiographic investigation of tooth renewal in purple sea urchin (*Strongylocentrotus purpuratus*). J Exp Zool 158:275–282

Huggins L, Lennarz WJ (2001) Inhibition of procollagen C-terminal proteinase blocks gastrulation and spicule elongation in the sea urchin embryo. Dev Growth Differ 43:415–424

Hyman LH (1955) The invertebrates: echinodermata. McGraw-Hill, New York

Ingersoll EP, Wilt FH (1998) Matrix metalloproteinase inhibitors disrupt spicule formation by primary mesenchyme cells in the sea urchin embryo. Dev Biol 196:95–106

Ingersoll E, Wilt F, MacDonald K (2003) The ultrastructural localization of SM30 and SM50 in the developing sea urchin embryo. J Exp Zool 300:101–112

Killian CE, Wilt FH (1996) Characterization of the proteins comprising the integral marix of embryonic spicules of *Strongylocentrotus purpuratus*. J Biol Chem 271:9150–9155

Killian CE, Wilt FH (2008) Molecular aspects of biomineralizatiionn of the echinoderm endoskeleton. Chem Rev 108:4463–4474

Killian CE, Metzler RA, Gong YT, Olson IC, Aizenberg J, Politi Y, Addadi L, Weiner S, Wilt FH, Scholl A, Young A, Doran A, Kunz M, Tamura N, Coppersmith SN, Gilbert PUPA (2009) The mechanism of calcite co-orientation in the sea urchin tooth. J Am Chem Soc 131:18404–18409

Killian CE, Croker L, Wilt FH (2010) SpSM30 gene family expression patterns in embryonic and adult biomineralized tissues of the sea urchin, *Strongylocentrotus purpuratus*. Gene Expr Patterns 10(2–3):135–139

Killian CE, Metzler RA, Gong YUT, Churchill TH, Olson IC, Trubetskoy V, Christensen MB, Fournelle JH, De Carlo F, Cohen S, Mahamid J, Wilt FH, Scholl A, Young A, Doran A, Coppersmith SN, Gilbert PUPA (2011) Self-sharpening mechanism of the sea urchin tooth. Adv Funct Mater 21:682–690

Kniprath E (1974) Ultrastructure and growth of the sea urchin tooth. Calc Tiss Res 14:211–228

Kudo M, Kameda J, Saruwatari K, Ozaki N, Okano K, Nagasawa H, Kogure T (2010) Microtexture of larval shell of oyster, *Crassostrea nippona*: a FIB-TEM study. J Struct Biol 169:1–5

Laubichler MD, Davidson EH (2008) Boveri's long experiment: sea urchin merogones and the establishment of the role of nuclear chromosomes in development. Dev Biol 314:1–11

Livingston BT, Killian C, Wilt FH, Cameron AC, Landrum MJ, Ermolaeva O, Sapojnikov V, Maglott DR, Ettensohn C (2006) A genome-wide analysis of biomineralization-related proteins in the sea urchin, *Strongylocentrotus purpuratus*. Dev Biol 300:335–348

Lowenstam H, Weiner S (1989) On biomineralization. Oxford University Press, New York

Ma Y, Weiner S, Addadi L (2007) Mineral deposition and crystal growth in the continuously forming teeth of sea urchins. Adv Funct Mater 17:2693–2700

Ma Y, Cohen SR, Addadi L, Weiner S (2008) Sea urchin tooth design: an "all-calcite" polycrystalline reinforced fiber composite for grinding rocks. Adv Mater 20:1555–1559

Ma Y, Aichmayer B, Paris O, Fratzl P, Meibom A, Metzler RA, Politi Y, Addadi L, Gilbert PUPA, Weiner S (2009) The grinding tip of the sea urchin tooth exhibits exquisite control over calcite crystal orientation and Mg distribution. Proc Natl Acad Sci USA 106:6048–6053

Magdans U, Gies H (2004) Single crystal structure analysis of sea urchin spine calcites. Eur J Miner 16:261–268

Mahamid J, Sharir A, Addadi L, Weiner S (2008) Amorphous calcium phosphate is a major component of the forming fin bones of zebrafish: indications for an amorphous precursor phase. Proc Natl Acad Sci USA 105:12748–12753

Mann K, Poustka AJ, Mann M (2008a) The sea urchin (*Strongylocentrotus purpuratus*) test and spine proteomes. Proteome Sci 6:22–32

Mann K, Proustka AJ, Mann M (2008b) In-depth, high-accuracy proteomics of sea urchin tooth organic matrix. Proteome Sci 6:33–44

Mann K, Poustka AJ, Wilt FH (2010) The sea urchin (*Strongylocentrotus purpuratus*) spicule proteome. Proteome Sci 8:33

Mann K, Wilt FH, Poustka AJ (2010) Proteomic analysis of sea urchin (*Strongylocentrotus purpuratus*) spicule matrix. Proteome Science 8

Märkel K, Titschack H (1969) Morphology of sea-urchin teeth (in German). Z Morph Tiere 64:179–200

Märkel K, Röser U (1983a) The spine tissues in the Echinoid *Eucidaris tribuloides*. Zoomorphology 103:25–41

Märkel K, Röser U (1983b) Calcite-resorption in the spine of the Echinoid *Eucidaris tribuloides*. Zoomorphology 103:43–58

McMahon SA, Miller JI, Lawton JA, Kerkow DE, Hodes A, Marti-Renom MKA, Doulatov S, Narayaanan E, Sali A, Miller JF, Ghosh P (2005) The C-type lectin fold as an evolutionary solution for massive sequence variation. Nat Struct Mol Biol 12:886–892

Metzler RA, Evans JS, Killian CE, Zhou D, Churchill TH, Appathurai NP, Coppersmith SN, Gilbert PUPA (2010) Nacre protein fragment templates lamellar aragonite growth. J Am Chem Soc 132:6329–6334

Michel FM, MacDonald J, Feng J, Phillips BL, Ehm L, Tarabrella C, Parise JB, Reeder RJ (2008) Structural characteristics of synthetic amorphous calcium carbonate. Chemistry of Materials 20:4720–4728

Mitsunaga K, Makihara R, Fujino Y, Yasumasu I (1986) Inhibitory effects of ethacrynic acid, furosemide and ifedipne on the calcification of spicules in cultures of micromeres from *H. pulcherrimus*. Differentiation 30:197–205

Moore HB (1966) Ecology of echinoids. In: Boolootian RA (ed) Physiology of echinodermata. John Wiley and Sons, New York, pp. 75–86

Moureaux C, Pérez-Huerta A, Compère P, Zhu W, Leloup T, Cusack M, Dubois P (2010) Structure, composition and mechanical relations to function in sea urchin spine. J Struct Biol 170(1):41–49

Nakano E, Okazaki K, Iwamatsu T (1963) Accumulation of radioactive calcium in larvae of the sea urchin *Pseudocentrotus depressus*. Biol Bull 125:125–133

Nassif N, PInna N, Gehrke N, antoniettei M, Jager C, Colfen H (2005) Amorphous layer around aragonite platelets in nacre. Proc Natl Acad Sci USA 102:12653–12655

Nelson BV, Vance RR (1979) Diel foraging patterns of the sea urchin *Centrostephanus coronatu*s as a predator avoidance strategy. Mar Biol 51:251–258

Okazaki K (1956) Skeleton formation of the sea urchin larvae. I. Effect of Ca concentration of the medium. Biol Bull 110:320–333

Okazaki K (1960) Skeleton formation of sea urchin larvae. II. Organic matrix of the spicule. Embryologia 5:283–320

Okazaki K (1975a) Spicule formation by isolated micromeres of the sea urchin embryo. Amer Zool 15:567–581

Okazaki K (1975b) Normal development to metamorphosis. In: Czihak G (ed) The sea urchin embryo. Springer, Berlin, pp 177–216

Okazaki K, Inoue S (1976) Crystal property of the larval sea urchin spicule. Dev Growth Differ 188:567–581

Orme CA, Noy A, Wierzbicki A, McBride MT, Grantham M, Teng HH, Dove PM, DeYoreo JJ (2001) Formation of chiral morphologies through selective binding of amino acids to calcite surface steps. Nature 411:775–779

Otter GW (1932) Rock burrowing echinoids. Biol Rev Camb Philos Soc 7:89–107

Peled-Kamar M, Hamilton P, Wilt FH (2002) The Spicule matrix protein LSM34 is essential for biomineralization of the sea urchin spicule. Exp Cell Res 272:56–61

Penn RL, Banfield JF (1999) Morphology development and crystal growth in nanocrystalline aggregates under hydrothermal conditions: Insights from titania. Geochim Cosmochim Acta 63:154915–154957

Politi Y, Arad T, Klein E, Weiner S, Addadi L (2004) Sea urchin spine calcite forms via a transient amorphous calcium carbonate phase. Science 306:1161–1164

Politi Y, Levi-Kalisman Y, Raz S, Wilt F, Addadi L, Weiner S, Sagi I (2006) Structural characterization of the transient amorphous calcium carbonate precursor phase in sea urchin embryos. Adv Funct Mater 16:1289–1298

Politi Y, Metzler RA, Abrecht M, Gilbert B, Wilt FH, Sagi I, Addadi L, Weiner S, Gilbert PUPA (2008) Transformation mechanism of amorphous calcium carbonate into calcite in the sea urchin larval spicule. Proc Natl Acad Sci USA 105:17362–17366

Radha AV, Forbes TZ, Killian CE, Gilbert PUPA, Navrotsky A (2010) Transformation and crystallization energetics of synthetic and biogenic amorphous calcium carbonate. Procs Natl Acad Sci USA 107:16438–16443

Raup DM (1966) The endoskeleton. In: Boolootian RA (ed) Physiology of echinodermata. John Wiley and Sons, New York, pp 379–395

Robach JS, Stock SR, Veis A (2009) Structure of first-and second-stage mineralized elements in teeth of the sea urchin *Lytechinus variegatus*. J Struct Biol 168:452–466

Seto J, Zhang Y, Hamilton P, Wilt F (2004) The localization of occluded matrix proteins in calcareous spicules of sea urchin larvae. J Struct Biol 148:123–130

Simkiss K, Wilbur KM (1989) Biomineralization. Academic Press, San Diego
Smith MM, Smith LC, Cameron RA, Urry L (2008) A larval staging scheme for *Strongylocentrotus purpuratus*. J Morphol 269:713–733
Veis A (2008) Crystals and life: an introduction. In: Sigel A, Sigel H, Sigel RKO (eds) Biomineralization. From nature to application, vol. 4 of metal ions in life sciences. John Wiley and Sons, Ltd, Chichester, pp 2–35
Wang RZ (1998) Fracture toughness and interfacial design of a biological fiber-matrix ceramic composite in sea urchin teeth. J Am Ceram Soc 81:1037–1040
Wang RZ, Addadi L, Weiner S (1997) Design strategies of sea urchin teeth: structure, composition and micromechanical relations to function. Phil Trans R Soc Lond B 352:469–480
Weiss I, Tuross N, Addadi L, Weiner S (2002) Mollusc larval shell formation: amorphous calcium carbonate is a precursor for aragonite. J Exp Zool A 293:478–491
Wilt FH (1999) Matrix and mineral in the sea urchin larval skeleton. J Struct Biol 126:216–226
Wilt FH (2002) Biomineralization of the spicules of sea urchin embryos. Zool Sci 19:253–261
Wilt FH, Ettensohn CE (2007) Morphogenesis and biomineralization of the sea urchin larval endoskeleton. In: Baeuerlein E (ed) Handbook of biomineralization. Wiley-VCH, Weinheim, pp 183–210
Wilt FH, Killian CE (2008) What genes and genomes tell us about calcium carbonate biomineralization. In: Sigel A, Sigel H, Sigel RKO (eds) Biomineralization. From nature to application, vol. 4 of metal ions in life sciences. John Wiley and Sons, Ltd, Chichester, pp 36–69
Wilt FH, Killian CE, Livingstson B (2003) Development of calcareous skeletal elements in invertebrates. Differentiation 71:237–250
Wilt FH, Killian CE, Hamilton P, Croker L (2008a) The dynamics of secretion during sea urchin embryonic skeleton formation. Exp Cell Res 314:1744–1752
Wilt FH, Croker L, Killian CE, McDonald K (2008b) Role of LSM34/SpSM50 proteins in endoskeletal spicule formation in sea urchin embryos. Invert Biol 127:452–459
Yajima M (2007) A switch in the cellular basis of skeletogenesis in late-stage sea urchin larvae. Dev Biol 307:272–281
Yajima M, Kiyomoto M (2006) Study of larval and adult skeletogenic cells in developing sea urchin larvae. Biol Bull 211:183–192
Yang L, Killian CE, Kunz M, Tamura N, Gilbert PUPA (2011) Biomineral nanoparticles are space-filling. RSC-Nanoscale 3:603–609
Zhu X, Mahairas G, Illies M, Cameron RA, Davidson EH, Ettensohn CA (2001) A large scale analysis of the mRNAs expressed by primary mesenchyme cells of the sea urchin embryo. Development 128:2615–2627